

**Bogoliubov dynamics of condensate collisions using the positive- $P$  representation**P. Deuar,<sup>1</sup> J. Chwedeńczuk,<sup>2</sup> M. Trippenbach,<sup>2</sup> and P. Ziń<sup>3</sup><sup>1</sup>*Institute of Physics, Polish Academy of Sciences, Al. Lotników 32/46, PL-02-668 Warsaw, Poland*<sup>2</sup>*Institute of Theoretical Physics, Physics Department, University of Warsaw, Hoża 69, PL-00-681 Warsaw, Poland*<sup>3</sup>*The Andrzej Sołtan Institute for Nuclear Studies, Hoża 69, PL-00-681 Warsaw, Poland*

(Received 6 May 2011; published 20 June 2011)

We formulate the time-dependent Bogoliubov dynamics of colliding Bose-Einstein condensates in terms of a positive- $P$  representation of the Bogoliubov field. We obtain stochastic evolution equations for the field which converge to the full Bogoliubov description as the number of realizations grows. The numerical effort grows linearly with the size of the computational lattice. We benchmark the efficiency and accuracy of our description against Wigner distribution and exact positive- $P$  methods. We consider its regime of applicability, and show that it is the most efficient method in the common situation when the total particle number in the system is insufficient for a truncated Wigner treatment.

DOI: [10.1103/PhysRevA.83.063625](https://doi.org/10.1103/PhysRevA.83.063625)

PACS number(s): 03.75.Nt, 05.30.-d, 34.50.Cx

**I. INTRODUCTION**

The collision of two Bose-Einstein condensates (BECs)—if the relative velocity is sufficiently high—leads to the formation of a halo of scattered atoms. This phenomenon has been the object of numerous experimental [1–17] and theoretical investigations [1,10,17–34]. The atoms forming the halo could be used for precision measurements [35], interferometry [2,36–39], or tests of quantum mechanics [40]. Condensate collisions are also related to such phenomena as molecular dissociation [41–56], atomic four-wave mixing [6,14,57–60], super-radiant scattering [61–70], atomic parametric down-conversion [71–77], and the impact of a BEC on a barrier [78–81].

Recently, in a series of experimental studies [1,2], a quantitative analysis of the supersonic collisions of two Bose-Einstein condensates was presented. It was based on stochastic Bogoliubov equations for a particle field interacting via a contact potential. In this paper we provide the details of that method. It relies on solving a set of stochastic equations in a plane-wave basis, rather than a diagonalization of the Hamiltonian. We have found this approach to be more effective as it allows one to study large-scale multimode problems that *would not be possible* with direct diagonalization. This is because in phase-space stochastic methods, such as those presented in this work, the computational requirements (memory, time) scale linearly with the number of modes or grid points.

Several stochastic methods have been used with success in the past to study the scattered atoms in these systems. They treated the full atom-field—in contrast to the Bogoliubov expansion applied here—using the truncated Wigner [23,26,28,33] and the positive- $P$  representations [17,28,29,32,33]. However, these are not suitable for a majority of current experiments, including the recent metastable helium condensate collisions [1,2,11,12,17,30]. The truncated Wigner approach is limited to the case when the total number of atoms in the system is much larger than the number of necessary modes [26,82,83], otherwise, significant discrepancies (“truncation”) with full quantum dynamics appear. The positive- $P$  approach is complete, but has numerical instabilities that make it useful

only for short times [28,33,84], often shorter than the duration of the collision.

Instead of a full atom-field approach, a wide class of collisions is described accurately by a Bogoliubov description. This approach is valid while the number of particles scattered during the collision is small in comparison with the total, a condition satisfied in most of the experiments. The time-adaptive refinement, where the condensate wave function undergoes mean-field evolution, is sufficient to describe most collision experiments. Moreover, contrary to a common fallacy, the Bogoliubov formulation takes into account the later Bose enhancement and stimulated scattering into quasiparticle modes that can occur.

The drawback of the Bogoliubov method has been that an accurate description of the real experimental situation typically requires a computational grid with  $10^6$ – $10^7$  points. A major contributing factor to this large lattice size is the need to resolve the supersonic wavelengths in the whole collision region. This large lattice renders a direct solution of the Bogoliubov–de Gennes evolution equations impossible. To avoid the diagonalization, one can introduce a phase-space distribution for the Bogoliubov field. We call this approach stochastic time-adaptive Bogoliubov (STAB). Here we use a positive- $P$  representation of the scattered particles, which differs from a previous well-known stochastic formulation [85], which used a Wigner representation. As is demonstrated below, the advantage of the present method is a much better signal-to-noise ratio in the calculations for most typical regimes of interest. As our positive- $P$ -based method is based on the broken-symmetry Bogoliubov description, it is applicable when the scattered particles are well separated in momentum space from condensates. This is the case for a wide range of supersonic phenomena, which apart from condensate collisions include molecular dissociation, super-radiant scattering, and parametric down-conversion, as well as supersonic flow past barriers and other impurities [86–88].

The paper is organized as follows. Section II provides the Bogoliubov description of a BEC collision. Section III introduces its positive- $P$  representation, and describes the resulting stochastic evolution equations used for simulations. In Sec. IV we compare the accuracy and efficiency of this

positive- $P$  Bogoliubov method ( $P$ -STAB) with the prior truncated Wigner, positive- $P$ , and Wigner Bogoliubov (W-STAB) methods for several characteristic BEC collision examples. We conclude in Sec. V.

## II. COLLIDING CONDENSATES—THE BOGOLIUBOV DESCRIPTION

We consider a zero-temperature, single-species bosonic gas. As it is dilute, the interatomic interaction can be effectively reduced to a contact delta potential with strength  $g$ . The second quantized Hamiltonian reads

$$\hat{H} = \int d^3\mathbf{x} \hat{\Psi}^\dagger(\mathbf{x}) \left( -\frac{\hbar^2}{2m} \nabla^2 + V(\mathbf{x}) \right) \hat{\Psi}(\mathbf{x}) + \frac{g}{2} \int d^3\mathbf{x} \hat{\Psi}^\dagger(\mathbf{x}) \hat{\Psi}^\dagger(\mathbf{x}) \hat{\Psi}(\mathbf{x}) \hat{\Psi}(\mathbf{x}),$$

where  $m$  is the atomic mass,  $g = 4\pi\hbar^2 a_s/m$ , with  $a_s$  being the  $s$ -wave scattering length, and  $V(\mathbf{x})$  is the external trapping potential. The field operator  $\hat{\Psi}(\mathbf{x})$  annihilates an atom at position  $\mathbf{x}$  and satisfies the bosonic commutation relations.

In order to start the (half-) collision, a superposition of two counterpropagating mutually coherent atomic clouds is prepared by a Bragg pulse. Simultaneously, the trapping potential is turned off. The two fractions begin to move apart along the  $z$  axis with relative speed  $2v_{\text{rec}}$ , twice the atomic recoil velocity. We define a speed of sound using the density at the center of the initial condensate ( $n_{\text{max}}$ ), obtaining  $c_{\text{max}} = \sqrt{gn_{\text{max}}/m}$ . In the supersonic limit, when  $2v_{\text{rec}} \gtrsim c_{\text{max}}$ , superfluidity is lost and a certain portion of atoms is scattered incoherently out of the BECs, forming the *halo*. The main focus of experiments and theory are the properties of the atoms in this halo.

In the time-dependent Bogoliubov approach [we use the simpler U(1) symmetry-breaking variety], the field operator is split into

$$\hat{\Psi}(\mathbf{x}, t) = \phi(\mathbf{x}, t) + \hat{\delta}(\mathbf{x}, t), \quad (1)$$

where  $\phi(\mathbf{x}, t)$  is the condensate wave function normalized to  $N$ —the number of particles. Its dynamics is governed by the Gross-Pitaevskii (GP) equation

$$i\hbar \frac{d\phi(\mathbf{x}, t)}{dt} = \left[ -\frac{\hbar^2}{2m} \nabla^2 + g|\phi(\mathbf{x}, t)|^2 \right] \phi(\mathbf{x}, t). \quad (2)$$

The Bogoliubov field operator  $\hat{\delta}(\mathbf{x}, t)$  describes the “noncondensed particles,” and obeys the equation

$$i\hbar \frac{\partial \hat{\delta}(\mathbf{x}, t)}{\partial t} = \left[ -\frac{\hbar^2}{2m} \nabla^2 + 2g|\phi(\mathbf{x}, t)|^2 \right] \hat{\delta}(\mathbf{x}, t) + g\phi^2(\mathbf{x}, t) \hat{\delta}^\dagger(\mathbf{x}, t). \quad (3)$$

The derivation of this equation is standard and based on removing higher-order dependence on  $\hat{\delta}$  and  $\hat{\delta}^\dagger$ —equivalent to assuming that the influence of the Bogoliubov field on itself is negligible as compared to the influence of the condensate.

The initial state of the trapped BEC is a solution of the stationary GP equation

$$\mu\phi_0(\mathbf{x}) = \left[ -\frac{\hbar^2}{2m} \nabla^2 + V(\mathbf{x}) + g|\phi_0(\mathbf{x})|^2 \right] \phi_0(\mathbf{x}), \quad (4)$$

with chemical potential  $\mu$ . The Bragg pulse transforms the condensate wave function into

$$\phi(\mathbf{x}, 0) \propto \phi_0(\mathbf{x}) [e^{ik_0z} + e^{-ik_0z}] / \sqrt{2}, \quad (5)$$

where  $k_0 = mv_{\text{rec}}/\hbar$  is the wave vector associated with the recoil velocity. Neglecting quantum depletion, which is tiny in most cases, the state of the noncondensed particles is a vacuum, denoted by  $|0\rangle$ .

A common approach now would be to diagonalize Eq. (3) using a Bogoliubov transformation, and solve the resulting Bogoliubov–de Gennes equations. However, for many systems of interest one requires  $10^6$ – $10^7$  points in  $\mathbf{x}$  space, which prohibits such diagonalization.

Instead, we develop an equivalent stochastic description of Eq. (3) using the positive- $P$  representation. To obtain the dynamical equations, it is necessary to start from a Hamiltonian description. Equation (3), together with its conjugate, can be used to trace back the effective Hamiltonian for the Bogoliubov field,

$$\hat{H}_{\text{eff}} = \int d^3\mathbf{x} \hat{\delta}^\dagger(\mathbf{x}) \left( -\frac{\hbar^2}{2m} \nabla^2 \right) \hat{\delta}(\mathbf{x}) \quad (6a)$$

$$+ 2g \int d^3\mathbf{x} |\phi(\mathbf{x})|^2 \hat{\delta}^\dagger(\mathbf{x}) \hat{\delta}(\mathbf{x}) \quad (6b)$$

$$+ \frac{g}{2} \int d^3\mathbf{x} \phi(\mathbf{x})^2 \hat{\delta}^\dagger(\mathbf{x}) \hat{\delta}^\dagger(\mathbf{x}) + \text{H.c.} \quad (6c)$$

Line (6a) contains the kinetic energy of the noncondensed particles and line (6b) the interaction between condensate and noncondensate particles. Finally, line (6c) governs the transfer of atomic pairs from the BEC to the  $\hat{\delta}$  field.

## III. $P$ -STAB METHOD

### A. Positive- $P$ representation of the Bogoliubov field

We employ the positive- $P$  representation to expand the density matrix for the uncondensed field  $\hat{\delta}(\mathbf{x}, t)$  as a distribution  $P$  over local coherent states at each point  $\mathbf{x}$  in space,

$$\hat{\rho} = \int P[\psi, \tilde{\psi}] \hat{\Lambda}[\psi, \tilde{\psi}] \mathcal{D}^2\psi \mathcal{D}^2\tilde{\psi}, \quad (7a)$$

where the complex fields  $\psi(\mathbf{x})$  and  $\tilde{\psi}(\mathbf{x})$  are the amplitudes of the local off-diagonal coherent state projectors  $\hat{\Lambda}$ ,

$$\hat{\Lambda}[\psi, \tilde{\psi}] = \bigotimes_{\mathbf{x}} \hat{\Lambda}_{\mathbf{x}}(\psi(\mathbf{x}), \tilde{\psi}(\mathbf{x})).$$

$$= \mathcal{N} \exp \left[ \int \psi(\mathbf{x}) \hat{\delta}^\dagger(\mathbf{x}) d\mathbf{x} \right] |0\rangle \langle 0| \times \exp \left[ \int \tilde{\psi}(\mathbf{x})^* \hat{\delta}(\mathbf{x}) d\mathbf{x} \right]. \quad (7b)$$

with normalization  $\mathcal{N} = \exp[-\int \tilde{\psi}(\mathbf{x})^* \psi(\mathbf{x}) d\mathbf{x}]$ . The operator  $|0\rangle \langle 0|$  projects onto the vacuum state. As the numerical computation is made on a grid, the local projectors  $\hat{\Lambda}_{\mathbf{x}}$  take on the form

$$\hat{\Lambda}_{\mathbf{x}} = e^{\psi(\mathbf{x}) \hat{\delta}^\dagger(\mathbf{x}) \Delta V} |0\rangle \langle 0| e^{\tilde{\psi}(\mathbf{x})^* [\hat{\delta}(\mathbf{x}) - \psi(\mathbf{x})] \Delta V} \quad (7c)$$

$$= \frac{|\alpha\rangle_{\mathbf{x}} \langle \tilde{\alpha}|_{\mathbf{x}}}{\langle \tilde{\alpha}|_{\mathbf{x}} |\alpha\rangle_{\mathbf{x}}}, \quad (7d)$$

where  $\Delta V = \Delta x \times \Delta y \times \Delta z$  is the volume per grid point,  $\alpha = \psi(\mathbf{x})\sqrt{\Delta V}$ ,  $\tilde{\alpha} = \tilde{\psi}(\mathbf{x})\sqrt{\Delta V}$ , and  $|\alpha\rangle_{\mathbf{x}}$  is a coherent state at location  $\mathbf{x}$  with complex amplitude  $\alpha$ . We note that the

distribution  $P[\psi, \tilde{\psi}]$  contains complete information about the density matrix  $\hat{\rho}$ .

Since it is non-negative and real, it can be regarded as a probability distribution of the complex valued fields  $\psi(\mathbf{x})$  and  $\tilde{\psi}(\mathbf{x})$ . It is therefore *also* equivalent to a large ensemble of samples of the fields. Consequently, the state  $\hat{\rho}$  is reproduced by the set of  $\psi(\mathbf{x})$  and  $\tilde{\psi}(\mathbf{x})$  when the number of samples  $S$  tends to infinity. The assumption that the initial state of  $\hat{\delta}$  is the vacuum is represented as

$$\psi(\mathbf{x}, 0) = \tilde{\psi}(\mathbf{x}, 0) = 0. \quad (8)$$

### B. Dynamics

The quantum evolution of the state

$$i\hbar \frac{\partial \hat{\rho}}{\partial t} = [\hat{H}_{\text{eff}}, \hat{\rho}] \quad (9)$$

is equivalent to a partial differential equation for  $P$  [89–91,93], which can be derived using the operator identities

$$\hat{\delta}(\mathbf{x})\hat{\Lambda} = \psi(\mathbf{x})\hat{\Lambda}, \quad (10)$$

$$\hat{\delta}^\dagger(\mathbf{x})\hat{\Lambda} = \left[ \tilde{\psi}(\mathbf{x})^* + \frac{1}{\Delta V} \frac{\partial}{\partial \psi(\mathbf{x})} \right] \hat{\Lambda}, \quad (11)$$

$$\hat{\Lambda}\hat{\delta}^\dagger(\mathbf{x}) = \tilde{\psi}(\mathbf{x})^* \hat{\Lambda}, \quad (12)$$

$$\hat{\Lambda}\hat{\delta}(\mathbf{x}) = \left[ \psi(\mathbf{x}) + \frac{1}{\Delta V} \frac{\partial}{\partial \tilde{\psi}(\mathbf{x})^*} \right] \hat{\Lambda}. \quad (13)$$

These identities are used to convert the quantum operators in  $\hat{H}_{\text{eff}}$  inside Eq. (9) to partial derivatives. The resulting equation is of a Fokker-Planck type and it is well known that it can be rendered into a random walk of the samples of  $\psi(\mathbf{x})$  and  $\tilde{\psi}(\mathbf{x})$ —the Langevin equations—which in the Ito representation read

$$i\hbar \frac{d\psi(\mathbf{x}, t)}{dt} = \left\{ -\frac{\hbar^2}{2m} \nabla^2 + 2g|\phi(\mathbf{x}, t)|^2 \right\} \psi(\mathbf{x}, t) + g\phi(\mathbf{x}, t)^2 \tilde{\psi}(\mathbf{x}, t)^* + \sqrt{i\hbar g} \phi(\mathbf{x}, t) \xi(\mathbf{x}, t), \quad (14a)$$

$$i\hbar \frac{d\tilde{\psi}(\mathbf{x}, t)}{dt} = \left\{ -\frac{\hbar^2}{2m} \nabla^2 + 2g|\phi(\mathbf{x}, t)|^2 \right\} \tilde{\psi}(\mathbf{x}, t) + g\phi(\mathbf{x}, t)^2 \psi(\mathbf{x}, t)^* + \sqrt{i\hbar g} \phi(\mathbf{x}, t) \tilde{\xi}(\mathbf{x}, t). \quad (14b)$$

Here  $\xi(\mathbf{x}, t)$  and  $\tilde{\xi}(\mathbf{x}, t)$  are delta correlated, independent, real Gaussian stochastic noise fields with variances

$$\langle \xi(\mathbf{x}, t) \tilde{\xi}(\mathbf{x}', t') \rangle = 0, \quad (15)$$

$$\langle \xi(\mathbf{x}, t) \xi(\mathbf{x}', t') \rangle = \langle \tilde{\xi}(\mathbf{x}, t) \tilde{\xi}(\mathbf{x}', t') \rangle = \delta^{(3)}(\mathbf{x} - \mathbf{x}') \delta(t - t').$$

and zero mean. Numerically,  $\xi$  and  $\tilde{\xi}$  are usually approximated by real Gaussian random variables of variance  $1/(\Delta t \Delta V)$  that are independent at each point at the computational lattice, and at each time step of length  $\Delta t$ .

One important feature of Eqs. (14) is that, similarly to Eq. (3), they are *linear* in  $\psi$  and  $\tilde{\psi}$ . This way, the nonlinear instabilities, boundary term systematics [92,93] and finite-simulation-time issues [84] that may occur in direct positive- $P$  treatments of the full boson field are absent.

### C. Observables

Expectation values of any normal-ordered observable are evaluated using the positive- $P$  representation by substituting  $\hat{\delta}^\dagger \rightarrow \tilde{\psi}^*$  and  $\hat{\delta} \rightarrow \psi$  and calculating a stochastic average [93], denoted as  $\langle \cdot \rangle_{\text{st}}$ ,

$$\left\langle \prod_j \hat{\delta}^\dagger(\mathbf{x}_j) \prod_k \hat{\delta}(\mathbf{x}_k) \right\rangle = \lim_{S \rightarrow \infty} \left\langle \prod_j \tilde{\psi}(\mathbf{x}_j)^* \prod_k \psi(\mathbf{x}_k) \right\rangle_{\text{st}}. \quad (16)$$

Note that since Eq. (3) is linear, and the initial state is vacuum, then at all times  $t$ ,

$$\langle 0 | \hat{\delta}(\mathbf{x}, t) | 0 \rangle = 0. \quad (17)$$

As an example, the one-particle density matrix is given by

$$\begin{aligned} \rho_1(\mathbf{x}, \mathbf{x}', t) &= \langle \hat{\Psi}^\dagger(\mathbf{x}, t) \hat{\Psi}(\mathbf{x}', t) \rangle \\ &= \phi(\mathbf{x}, t)^* \phi(\mathbf{x}', t) + \langle \hat{\delta}^\dagger(\mathbf{x}, t) \hat{\delta}(\mathbf{x}', t) \rangle \\ &\quad + \phi(\mathbf{x}, t)^* \langle \hat{\delta}(\mathbf{x}', t) \rangle + \phi(\mathbf{x}', t) \langle \hat{\delta}^\dagger(\mathbf{x}, t) \rangle \\ &= \phi(\mathbf{x}, t)^* \phi(\mathbf{x}', t) + \langle \hat{\delta}^\dagger(\mathbf{x}, t) \hat{\delta}(\mathbf{x}', t) \rangle \\ &= \phi(\mathbf{x}, t)^* \phi(\mathbf{x}', t) + \langle \tilde{\psi}(\mathbf{x}, t)^* \psi(\mathbf{x}', t) \rangle_{\text{st}}, \end{aligned}$$

where we used Eq. (17) on the second-to-last line. The number of noncondensed atoms is

$$\delta N = \int \langle \hat{\delta}^\dagger(\mathbf{x}) \hat{\delta}(\mathbf{x}) \rangle d^3 \mathbf{x} = \int \langle \tilde{\psi}(\mathbf{x})^* \psi(\mathbf{x}) \rangle_{\text{st}} d^3 \mathbf{x}. \quad (18)$$

For a general observable  $\hat{F}$ , the best estimate of its expectation value  $\langle \hat{F} \rangle$  is given by the mean of its corresponding estimator  $f(\psi, \tilde{\psi}, \phi)$ ,

$$\bar{F} = \langle f \rangle_{\text{st}}.$$

The uncertainty in this mean is best estimated via the variance of a set of subensemble means: We divide the  $S$  realizations into  $n$  bins of equal size  $s$  (so  $S = sn$ ), and the  $j$ th subensemble ( $j = 1, \dots, n$ ) gives a subensemble mean  $\bar{F}_j = \langle f \rangle_{\text{st}, j}$ . Due to the central limit theorem, these subensemble means are approximately normal distributed (which is not necessarily the case for the estimators from individual realizations). As a result, the uncertainty in the final mean ( $\bar{F} = \frac{1}{n} \sum_{j=1}^n \bar{F}_j$ ) also is well estimated by

$$\Delta F = \sqrt{\frac{\text{var}[\bar{F}_j]}{n-1}}. \quad (19)$$

### D. Orthogonality and applicability

It is well known that the U(1) symmetry-breaking Bogoliubov approach encounters some problems at long evolution times. These are related to an incomplete treatment of the phase spreading of the condensate [94]. As this approach does not preserve the orthogonality of the noncondensed field  $\hat{\delta}(\mathbf{x})$  with the condensate mode [95], the part of  $\hat{\delta}$  that accumulates atop the condensate could just as well be considered to still be part of the BEC, and discounted from the number of scattered particles.

For this reason, the results of the above method should be treated with caution when modes having significant overlap with the condensate are relevant. In practice, such modes lie

in parts of  $k$  space close to the condensate clouds. Fortunately, the bulk of the halo is well separated from the condensates and remains unaffected.

More generally, supersonicity always leads to orthogonality between scattered and condensed atoms because the condensate mode function contains no plane-wave components above the speed of sound. This allows the use of the method presented here for collisions of BECs, molecular dissociation, super-radiant scattering, parametric down-conversion, or flow past barriers and other impurities.

#### IV. RELATIONSHIP WITH COMPARABLE METHODS

Stochastic evolution equations have been previously derived for Bogoliubov descriptions of cold atom systems by Sinatra *et al.* [85] using the Wigner representation. An immediate question is how the positive- $P$ -based method presented here compares. We expect that the positive- $P$  method will tend to be inherently less “noisy” initially due to a lack of the starting noise that is necessary to represent the vacuum in the Wigner treatment. It is also instructive to compare performance and accuracy with the two other stochastic methods used previously (positive- $P$  and truncated Wigner) which treat the whole atom field  $\hat{\Psi}$  as one unit without using the Bogoliubov approximation. In this section we will benchmark these four simulation methods.

##### A. Wigner STAB

Representing the U(1) symmetry-breaking description of Sec. II using the Wigner representation we obtain the following stochastic description of the field  $\hat{\delta}(\mathbf{x})$ . There is only one complex field  $\psi_w(\mathbf{x})$ , with the initial vacuum described by a random initial condition that places half a virtual particle into each mode,

$$\psi_w(\mathbf{x}, 0) = \frac{\sqrt{\Delta t}}{2} [\xi(\mathbf{x}, 0) + i\tilde{\xi}(\mathbf{x}, 0)]. \quad (20)$$

[The noises  $\xi$  and  $\tilde{\xi}$  are as defined by Eq. (15)]. The subsequent evolution contains no noise and is

$$i\hbar \frac{d\psi_w(\mathbf{x}, t)}{dt} = \left\{ -\frac{\hbar^2}{2m} \nabla^2 + 2g|\phi(\mathbf{x}, t)|^2 \right\} \psi_w(\mathbf{x}, t) + g\phi(\mathbf{x}, t)^2 \psi_w(\mathbf{x}, t)^*. \quad (21)$$

Observable calculations differ somewhat because the half-particle occupation of the initial modes must be corrected for. For example,

$$\rho_1(\mathbf{x}, \mathbf{x}', t) = \phi(\mathbf{x}, t)^* \phi(\mathbf{x}', t) + \langle \psi_w(\mathbf{x}, t)^* \psi_w(\mathbf{x}', t) \rangle_{st} - \frac{1}{2} \delta(\mathbf{x} - \mathbf{x}'). \quad (22)$$

This is the symmetry-breaking analog of the more involved number-conserving description of Sinatra *et al.* [85] and shares the same noise properties. However, the same orthogonality caveats (Sec. III D) apply as for the  $P$ -STAB method derived in this paper.

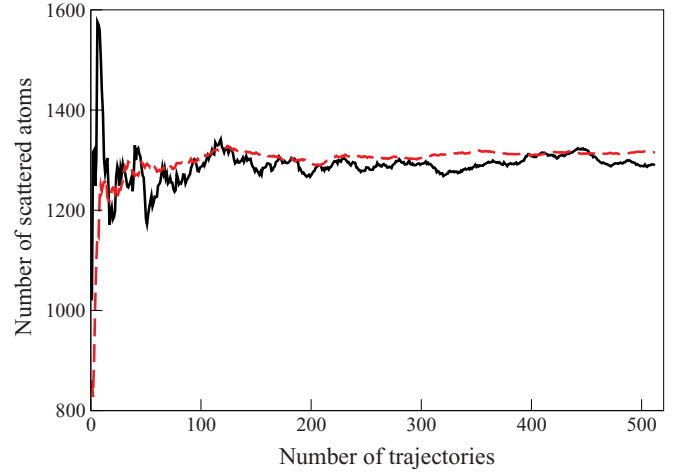


FIG. 1. (Color online) The convergence of observable estimates in the two Bogoliubov methods as the number of trajectories is increased. The system is the  $^4\text{He}$  collision of [1]. The quantity shown is the total number of atoms in the halo at  $t = 120 \mu\text{s}$ , well after the end of the collision. Narrow  $k$ -space regions containing the condensates were excluded from the atom sum. Black solid line: Wigner Bogoliubov calculation (W-STAB); red dashed line: positive- $P$  Bogoliubov (P-STAB).

##### B. Full-field methods

For some parameters, another good alternative is to use the truncated Wigner representation to simulate the complete boson field directly, as was done by Norrie *et al.* [23,26]. This has the advantage of being applicable beyond the undepleted source approximation. However, the total number of particles should be significantly larger than the number of modes (for correctness [26,28]). This approach requires the truncation of some high-order terms in the partial differential equation for the resulting phase-space distribution  $P$ , leading to the name “truncated” Wigner representation. Here there is one complex field  $\psi_w(\mathbf{x})$  [no separate condensate field  $\phi(\mathbf{x}, t)$ ] with the initial state

$$\psi_w(\mathbf{x}, 0) = \phi(\mathbf{x}, 0) + \frac{\sqrt{\Delta t}}{2} [\xi(\mathbf{x}, 0) + i\tilde{\xi}(\mathbf{x}, 0)]. \quad (23)$$

The subsequent evolution contains no noise and is

$$i\hbar \frac{d\psi_w(\mathbf{x}, t)}{dt} = \left\{ -\frac{\hbar^2}{2m} \nabla^2 + g|\psi_w(\mathbf{x}, t)|^2 \right\} \psi_w(\mathbf{x}, t). \quad (24)$$

The one-particle density matrix is given by

$$\rho_1(\mathbf{x}, \mathbf{x}', t) = \langle \psi_w(\mathbf{x}, t)^* \psi_w(\mathbf{x}', t) \rangle_{st} - \frac{1}{2} \delta(\mathbf{x} - \mathbf{x}'). \quad (25)$$

Finally, a direct treatment of the full field using the positive- $P$  representation has been used [17,28,29,32,33]. Here there are two complex fields  $\psi_p(\mathbf{x})$  and  $\tilde{\psi}_p(\mathbf{x})$  with the initial state

$$\psi_p(\mathbf{x}, 0) = \tilde{\psi}_p(\mathbf{x}, 0) = \phi(\mathbf{x}, 0). \quad (26)$$

The evolution is

$$i\hbar \frac{d\psi_p(\mathbf{x}, t)}{dt} = \left\{ -\frac{\hbar^2}{2m} \nabla^2 + g\tilde{\psi}_p(\mathbf{x}, t)^* \psi_p(\mathbf{x}, t) + \sqrt{i\hbar g} \xi(\mathbf{x}, t) \right\} \psi_p(\mathbf{x}, t), \quad (27)$$

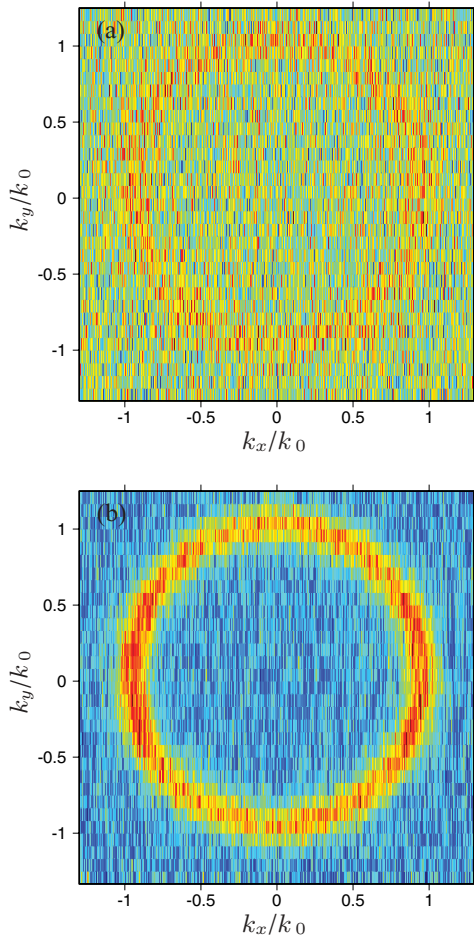


FIG. 2. (Color online) Slices of the halo density on the plane  $k_z = 0$ , perpendicular to the collision direction, for the  $^4\text{He}$  collision of [1].  $t = 48 \mu\text{s}$ , right at the end of the collision. Both results are from ensembles of 224 realizations. (a) Wigner Bogoliubov; (b) positive- $P$  Bogoliubov.

$$i\hbar \frac{d\tilde{\psi}_p(\mathbf{x}, t)}{dt} = \left\{ -\frac{\hbar^2}{2m} \nabla^2 + g\psi_p(\mathbf{x}, t)^* \tilde{\psi}_p(\mathbf{x}, t) + \sqrt{i\hbar g} \tilde{\xi}(\mathbf{x}, t) \right\} \tilde{\psi}_p(\mathbf{x}, t). \quad (28)$$

The one-particle density matrix is calculated with

$$\rho_1(\mathbf{x}, \mathbf{x}', t) = \langle \tilde{\psi}_p(\mathbf{x}, t)^* \tilde{\psi}_p(\mathbf{x}', t) \rangle_{st}. \quad (29)$$

### C. Efficiency measures

When considering the halo, the most pertinent observables have been the total number of particles, the density distribution in  $k$  space, and density correlations between specified regions in the halo. Accuracy in the latter two kinds of observables hinge on a good signal-to-noise ratio of the local density in  $k$  space. The uncertainty of the final estimates is given by Eq. (19), a function of the ratio between variance of the estimator and the number of realizations  $S \propto n$ . So, other things being equal, the computational effort required to achieve a set accuracy will scale as that variance. Accordingly, in Figs. 3 and 4 (upper panels) we will show how the variance

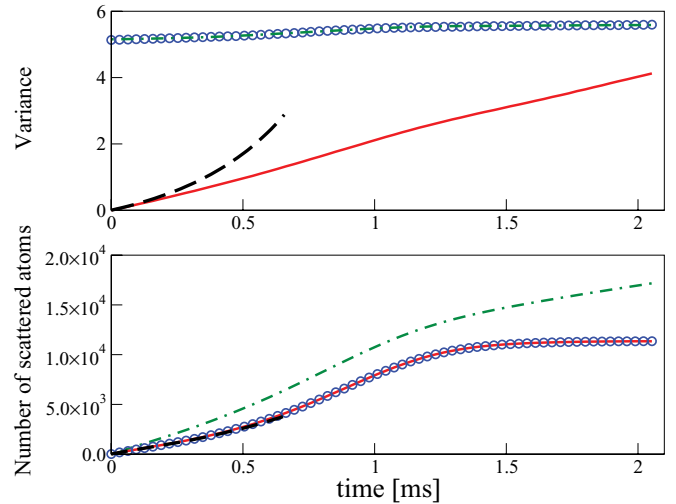


FIG. 3. (Color online)  $^{23}\text{Na}$  BEC collision as in [28,32,33].  $N = 1.5 \times 10^5$ . Upper panel: Variances of local atom density estimators in the slice at  $k_z = 0$  obtained for various methods, as for use in Eq. (19)—see text. An average value over all  $k_x$  and  $k_y$  locations in the slice is shown. Lower panel: Number of scattered atoms in the halo. Solid red line: positive- $P$  Bogoliubov simulation as described in this paper; blue circles: Wigner Bogoliubov simulation; dot-dashed green line: truncated Wigner simulation; dashed black line: positive- $P$  simulation of the full field.

of the estimators of halo density in  $k$  space compare between methods as a function of time. In Figs. 1 and 2 we directly show the noise that is seen with the full-field positive- $P$  and Wigner Bogoliubov treatments.

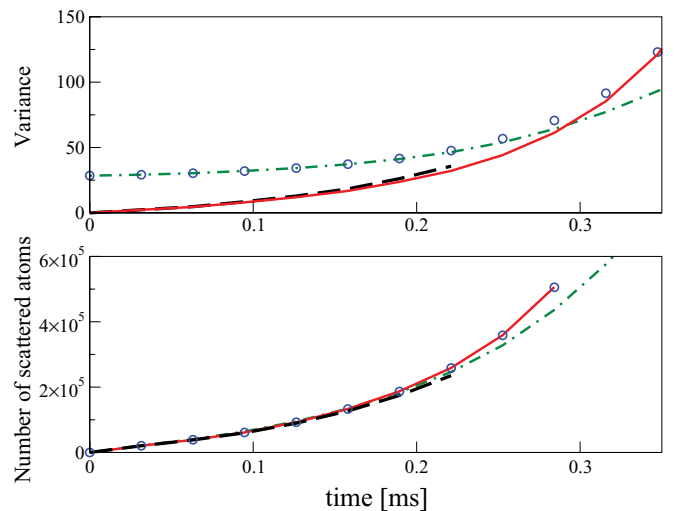


FIG. 4. (Color online)  $^{23}\text{Na}$  BEC collision with the same parameters as used in [23].  $N = 6 \times 10^6$ . Upper panel: Variances of local atom density estimators in the slice at  $k_z = 0$  obtained for various methods, as for use in Eq. (19)—see text. An average value over all  $k_x$  and  $k_y$  locations in the slice is shown. Lower panel: Number of scattered atoms in the halo. Solid red line: positive- $P$  Bogoliubov simulation as described in this paper; blue circles: Wigner Bogoliubov simulation; dot-dashed green line: truncated Wigner simulation; dashed black line: positive- $P$  simulation of the full field. The Bogoliubov simulations were stopped when the depletion reached 10%.

#### D. The low and moderate particle number case

Let us first consider the common case when the total number of atoms in the halo is quite low—so low that the number of halo atoms per mode is much less than one. Here we expect the initial noise in the Wigner methods (20) or (23) to be a severe problem, since the initial atom number variance there is  $1/2$  per mode, regardless of how many true atoms are present.

The first plots (Figs. 1 and 2) are from Wigner and positive- $P$  Bogoliubov simulations using the experimental parameters of [1], which described the collision of a BEC of metastable  $^4\text{He}^*$  atoms. They show the amount of noisiness in observables after the end of the collision. In this case, no bosonic enhancement of the scattering process occurred, thus the total number of atoms in the halo was quite low ( $\approx 1300$ ), while the number of modes was  $2.95 \times 10^6$ .

The next figure, Fig. 3, shows the halo density variance and the total number of scattered atoms in the collision of a BEC of  $150\,000$   $^{23}\text{Na}$  atoms. This case was considered in several previous works [28,32,33]. Here the halo reached  $1.1 \times 10^4$  atoms with  $1.08 \times 10^6$  modes.

We see that the noise in the Wigner calculations is severe in these cases, as compared to the positive- $P$  methods. Although the noise in the  $P$ -STAB calculation grows with time, it never surpasses the level of the Wigner methods for the time scales shown. The variance in both Wigner methods is identical.

The lower panel of Fig. 3 shows the accuracy of the methods. Both Bogoliubov methods agree perfectly with each other and with the exact calculation that uses the positive- $P$  representation of the full field (for as long as it lasts). The truncated Wigner displays a false growth of the number of particles in the halo. This is due to known spurious scattering by virtual particles when the momentum cutoff is this large, as described in [28,33,82]. For this simulation, the number of spatial modes is much larger than the number of true particles (150 000).

#### E. The high particle number case

A different situation is presented in Fig. 4, where we used the parameters from [23], where  $6 \times 10^6$  atoms of  $^{23}\text{Na}$  participated in the collision. There were  $3.14 \times 10^6$  spatial modes. As the final depletion of the condensate is large (about 40%), the Bogoliubov calculation was stopped at  $t \approx 280 \mu\text{s}$ , when the depletion reached 10%. Indeed, in the lower panel of Fig 4, one sees a difference beginning to appear between the two simulations at this time. In comparison, significant dynamics lasts until  $\approx 1000 \mu\text{s}$  (not shown).

The noise performance of the  $P$ -STAB method is superior here only for  $t \lesssim 300 \mu\text{s}$ . However, this still matches the entire period when the Bogoliubov description is accurate.

### V. CONCLUSIONS

We have developed the above positive- $P$  Bogoliubov stochastic simulation method for use with cold atom gases

and benchmarked it with existing approaches. As with other phase-space methods, it lends itself to simulation of quite general systems, as the calculation is carried out on a simple rectangular grid in  $x/k$  space, and individual realizations are run independently of each other. The computational complexity involved scales linearly with the size of the computational lattice used, allowing for up to  $\approx 10^7$  points in the lattice on a common workstation.

The method is applicable for a wide range of supersonic phenomena, its main validity conditions being (1) that the bulk of scattered atoms are well separated from the condensates in momentum space and (2) that the depletion of the original condensates can be neglected. The condensate wave function is, however, free to evolve in time. We note particularly that the method handles both spontaneous and stimulated scattering.

The positive- $P$  Bogoliubov method is superior in efficiency to the Wigner representation in almost all cases that we have seen where a  $U(1)$  symmetry-breaking Bogoliubov method can still be applied. However, one can imagine some long time situations where the Wigner simulation wins since, other things being equal, the variance in the positive- $P$  approach grows approximately linearly with time, while the variance in the Wigner method stays approximately constant around its initial, large value. (These trends are seen in the top panel of Fig. 3.) For situations where the overlap between the scattered and condensate field is non-negligible the number-conserving Wigner method [85] can be used instead. For situations with large condensate depletion, there remain the truncated Wigner or positive- $P$  treatments of the full boson field.

A more robust positive- $P$  formulation that explicitly imposes orthogonality between condensate and quasiparticle modes as in the number-conserving Bogoliubov treatment [95] is under development and will be presented in a forthcoming work.

We did not make comparisons with experimental data here since such comparison has been made previously [1,2]. However, we do compare to the full field positive- $P$  method. It is equivalent to full many-body quantum calculations and as such it can be used as a reference for other theoretical calculations.

### ACKNOWLEDGMENTS

It is a pleasure to thank Karen Kheruntsyan, Chris Westbrook, Denis Boiron, Nick Proukakis, Alice Sinatra, and Brian Dalton for valuable discussions on these matters. P.D. acknowledges support by the EU Contract No. PERG06-GA-2009-256291 and Polish Government Research Funds for the years 2010–2013; M.T. and P.Z. acknowledge support of Polish Government Research Grants for 2007–2011; J.Ch. was supported by Foundation for Polish Science International TEAM Programme cofinanced by the EU European Regional Development Fund.

[1] V. Krachmalnicoff *et al.*, *Phys. Rev. Lett.* **104**, 150402 (2010).  
 [2] J.-C. Jaskula, M. Bonneau, G. B. Partridge, V. Krachmalnicoff, P. Deuar, K. V. Kheruntsyan, A. Aspect, D. Boiron, and C. I. Westbrook, *Phys. Rev. Lett.* **105**, 190402 (2010).

[3] A. P. Chikkatur, A. Gorlitz, D. M. Stamper-Kurn, S. Inouye, S. Gupta, and W. Ketterle, *Phys. Rev. Lett.* **85**, 483 (2000).  
 [4] J. Steinhauer, R. Ozeri, N. Katz, and N. Davidson, *Phys. Rev. Lett.* **88**, 120407 (2002).

- [5] N. Katz, J. Steinhauer, R. Ozeri, and N. Davidson, *Phys. Rev. Lett.* **89**, 220401 (2002).
- [6] J. M. Vogels, K. Xu, and W. Ketterle, *Phys. Rev. Lett.* **89**, 020401 (2002).
- [7] J. M. Vogels, J. K. Chin, and W. Ketterle, *Phys. Rev. Lett.* **90**, 030403 (2003).
- [8] N. Katz, R. Ozeri, E. Rowen, E. Gershnel, and N. Davidson, *Phys. Rev. A* **70**, 033615 (2004).
- [9] C. Buggle, J. Leonard, W. von Klitzing, and J. T. M. Walraven, *Phys. Rev. Lett.* **93**, 173202 (2004).
- [10] N. Katz, E. Rowen, R. Ozeri, and N. Davidson, *Phys. Rev. Lett.* **95**, 220403 (2005).
- [11] A. Perrin, H. Chang, V. Krachmalnicoff, M. Schellekens, D. Boiron, A. Aspect, and C. I. Westbrook, *Phys. Rev. Lett.* **99**, 150405 (2007).
- [12] R. G. Dall, L. J. Byron, A. G. Truscott, G. R. Dennis, M. T. Johnsson, and J. J. Hope, *Phys. Rev. A* **79**, 011601(R) (2009).
- [13] M. Kozuma, L. Deng, E. W. Hagley, J. Wen, R. Lutwak, K. Helmerson, S. L. Rolston, and W. D. Phillips, *Phys. Rev. Lett.* **82**, 871 (1999).
- [14] L. Deng, E. W. Hagley, J. Wen, M. Trippenbach, Y. Band, P. S. Julienne, J. E. Simsarian, K. Helmerson, S. L. Rolston, and W. D. Phillips, *Nature (London)* **398**, 218 (1999).
- [15] P. Maddaloni, M. Modugno, C. Fort, F. Minardi, and M. Inguscio, *Phys. Rev. Lett.* **85**, 2413 (2000).
- [16] Y. B. Band, J. P. Burke, Jr., A. Simoni, and P. S. Julienne, *Phys. Rev. A* **64**, 023607 (2001).
- [17] A. Perrin, C. M. Savage, D. Boiron, V. Krachmalnicoff, C. I. Westbrook, and K. V. Kheruntsyan, *New J. Phys.* **10**, 045021 (2008).
- [18] Y. B. Band, M. Trippenbach, J. P. Burke, and P. S. Julienne, *Phys. Rev. Lett.* **84**, 5462 (2000).
- [19] M. Trippenbach, Y. B. Band, and P. S. Julienne, *Phys. Rev. A* **62**, 023608 (2000).
- [20] V. A. Yurovsky, *Phys. Rev. A* **65**, 033605 (2002).
- [21] R. Bach, M. Trippenbach, and K. Rzażewski, *Phys. Rev. A* **65**, 063605 (2002).
- [22] J. Chwedeńczuk, M. Trippenbach, and K. Rzażewski, *J. Phys. B* **37**, L391 (2004).
- [23] A. A. Norrie, R. J. Ballagh, and C. W. Gardiner, *Phys. Rev. Lett.* **94**, 040401 (2005).
- [24] P. Ziń, J. Chwedeńczuk, A. Veitia, K. Rzażewski, and M. Trippenbach, *Phys. Rev. Lett.* **94**, 200401 (2005).
- [25] P. Ziń, J. Chwedeńczuk, and M. Trippenbach, *Phys. Rev. A* **73**, 033602 (2006).
- [26] A. A. Norrie, R. J. Ballagh, and C. W. Gardiner, *Phys. Rev. A* **73**, 043617 (2006).
- [27] J. Chwedeńczuk, P. Zin, K. Rzażewski, and M. Trippenbach, *Phys. Rev. Lett.* **97**, 170404 (2006).
- [28] P. Deuar and P. D. Drummond, *Phys. Rev. Lett.* **98**, 120402 (2007).
- [29] P. D. Drummond, P. Deuar, and J. F. Corney, *Opt. Spectrosc.* **103**, 7 (2007).
- [30] J. Chwedeńczuk, P. Ziń, M. Trippenbach, A. Perrin, V. Leung, D. Boiron, and C. I. Westbrook, *Phys. Rev. A* **78**, 053605 (2008).
- [31] K. Molmer, A. Perrin, V. Krachmalnicoff, V. Leung, D. Boiron, A. Aspect, and C. I. Westbrook, *Phys. Rev. A* **77**, 033601 (2008).
- [32] M. Ögren and K. V. Kheruntsyan, *Phys. Rev. A* **79**, 021606(R) (2009).
- [33] P. Deuar, *Phys. Rev. Lett.* **103**, 130402 (2009).
- [34] Y. Wang, J. P. D’Incao, H.-C. Nagerl, and B. D. Esry, *Phys. Rev. Lett.* **104**, 113201 (2010).
- [35] H. A. Bachor and T. C. Ralph, *A Guide to Experiments in Quantum Optics*, 2nd ed. (Wiley-VCH, Berlin, 2004).
- [36] C. Gross, T. Zibold, E. Nicklas, J. Esteve, and M. K. Oberthaler, *Nature (London)* **464**, 1165 (2010).
- [37] P. Bouyer and M. A. Kasevich, *Phys. Rev. A* **56**, R1083 (1997).
- [38] J. A. Dunningham, K. Burnett, and S. M. Barnett, *Phys. Rev. Lett.* **89**, 150401 (2002).
- [39] R. A. Campos, C. C. Gerry, and A. Benmoussa, *Phys. Rev. A* **68**, 023810 (2003).
- [40] M. D. Reid, P. D. Drummond, W. P. Bowen, E. G. Cavalcanti, P. H. Lam, H. A. Bachor, U. L. Andersen, and G. Leuchs, *Rev. Mod. Phys.* **81**, 1727 (2009).
- [41] M. Ögren and K. V. Kheruntsyan, *Phys. Rev. A* **78**, 011602(R) (2008).
- [42] T. Mukaiyama, J. R. Abo-Shaeer, K. Xu, J. K. Chin, and W. Ketterle, *Phys. Rev. Lett.* **92**, 180402 (2004).
- [43] S. Dürr, T. Volz, and G. Rempe, *Phys. Rev. A* **70**, 031601(R) (2004).
- [44] M. Greiner, C. A. Regal, J. T. Stewart, and D. S. Jin, *Phys. Rev. Lett.* **94**, 110401 (2005).
- [45] U. V. Poulsen and K. Mølmer, *Phys. Rev. A* **63**, 023604 (2001).
- [46] K. V. Kheruntsyan and P. D. Drummond, *Phys. Rev. A* **66**, 031602(R) (2002).
- [47] K. V. Kheruntsyan, M. K. Olsen, and P. D. Drummond, *Phys. Rev. Lett.* **95**, 150405 (2005).
- [48] K. V. Kheruntsyan, *Phys. Rev. Lett.* **96**, 110401 (2006).
- [49] C. M. Savage, P. E. Schwenn, and K. V. Kheruntsyan, *Phys. Rev. A* **74**, 033620 (2006).
- [50] C. M. Savage and K. V. Kheruntsyan, *Phys. Rev. Lett.* **99**, 220404 (2007).
- [51] M. W. Jack and H. Pu, *Phys. Rev. A* **72**, 063625 (2005).
- [52] B. Zhao, Z.-B. Chen, J.-W. Pan, J. Schmiedmayer, A. Recati, G. E. Astrakharchik, and T. Calarco, *Phys. Rev. A* **75**, 042312 (2007).
- [53] I. Tikhonenkov and A. Vardi, *Phys. Rev. Lett.* **98**, 080403 (2007).
- [54] M. J. Davis, S. J. Thwaite, M. K. Olsen, and K. V. Kheruntsyan, *Phys. Rev. A* **77**, 023617 (2008).
- [55] M. Ögren, C. M. Savage, and K. V. Kheruntsyan, *Phys. Rev. A* **79**, 043624 (2009).
- [56] M. Ögren and K. V. Kheruntsyan, *Phys. Rev. A* **82**, 013641 (2010).
- [57] H. Pu and P. Meystre, *Phys. Rev. Lett.* **85**, 3987 (2000).
- [58] M. Trippenbach, Y. B. Band, and P. S. Julienne, *Opt. Express* **3**, 530 (1998).
- [59] L.-M. Duan, A. Sørensen, J. I. Cirac, and P. Zoller, *Phys. Rev. Lett.* **85**, 3991 (2000).
- [60] V. Boyer, A. M. Marino, R. C. Pooser, and P. D. Lett, *Science* **321**, 544 (2008).
- [61] A. Vardi and M. G. Moore, *Phys. Rev. Lett.* **89**, 090403 (2002).
- [62] S. Inouye, A. P. Chikkatur, D. M. Stamper-Kurn, J. Stenger, D. E. Pritchard, and W. Ketterle, *Science* **285**, 571 (1999).
- [63] M. G. Moore and P. Meystre, *Phys. Rev. Lett.* **83**, 5202 (1999).
- [64] A. Hilliard, F. Kaminski, R. le Targat, C. Olausson, E. S. Polzik, and J. H. Müller, *Phys. Rev. A* **78**, 051403(R) (2008).
- [65] D. Schneble, Y. Torii, M. Boyd, E. W. Streed, D. E. Pritchard, and W. Ketterle, *Science* **300**, 475 (2003).
- [66] L. E. Sadler, J. M. Higbie, S. R. Leslie, M. Vengalattore, and D. M. Stamper-Kurn, *Phys. Rev. Lett.* **98**, 110401 (2007).

- [67] D. Schneble, G. K. Campbell, E. W. Streed, M. Boyd, and D. E. Pritchard, and W. Ketterle, *Phys. Rev. A* **69**, 041601(R) (2004).
- [68] Y. Yoshikawa, T. Sugiura, Y. Torii, and T. Kuga, *Phys. Rev. A* **69**, 041603(R) (2004).
- [69] J. Li, X. Zhou, F. Yang, and X. Chen, *Phys. Lett. A* **372**, 4750 (2008).
- [70] L. F. Buchmann, G. M. Nikolopoulos, O. Zobay, and P. Lambropoulos, *Phys. Rev. A* **81**, 031606(R) (2010).
- [71] G. K. Campbell, J. Mun, M. Boyd, E. W. Streed, W. Ketterle, and D. E. Pritchard, *Phys. Rev. Lett.* **96**, 020406 (2006).
- [72] A. J. Ferris, M. K. Olsen, and M. J. Davis, *Phys. Rev. A* **79**, 043634 (2009).
- [73] L. Fallani, L. De Sarlo, J. E. Lye, M. Modugno, R. Saers, C. Fort, and M. Inguscio, *Phys. Rev. Lett.* **93**, 140406 (2004).
- [74] L. De Sarlo, L. Fallani, J. E. Lye, M. Modugno, R. Saers, C. Fort, and M. Inguscio, *Phys. Rev. A* **72**, 013603 (2005).
- [75] N. Gemelke, E. Sarajlic, Y. Bidel, S. Hong, and S. Chu, *Phys. Rev. Lett.* **95**, 170404 (2005).
- [76] K. M. Hilligsøe and K. Mølmer, *Phys. Rev. A* **71**, 041602(R) (2005).
- [77] K. Mølmer, *New J. Phys.* **8**, 170 (2006).
- [78] R. G. Scott, D. A. W. Hutchinson, and C. W. Gardiner, *Phys. Rev. A* **74**, 053605 (2006).
- [79] R. G. Scott, C. W. Gardiner, and D. A. W. Hutchinson, *Laser Phys.* **17**, 527 (2007).
- [80] T. A. Pasquini, Y. Shin, C. Sanner, M. Saba, A. Schirotzek, D. E. Pritchard, and W. Ketterle, *Phys. Rev. Lett.* **93**, 223201 (2004).
- [81] T. A. Pasquini, M. Saba, G.-B. Jo, Y. Shin, W. Ketterle, D. E. Pritchard, T. A. Savas, and N. Mulders, *Phys. Rev. Lett.* **97**, 093201 (2006).
- [82] A. Sinatra, C. Lobo, and Y. Castin, *J. Phys. B* **35**, 3599 (2002).
- [83] P. B. Blakie, A. S. Bradley, M. J. Davis, R. J. Ballagh, and C. W. Gardiner, *Adv. Phys.* **57**, 363 (2008).
- [84] P. Deuar and P. D. Drummond, *J. Phys. A* **39**, 1163 (2006).
- [85] A. Sinatra, Y. Castin, and C. Lobo, *J. Mod. Opt.* **47**, 2629 (2000).
- [86] R. G. Scott and D. A. W. Hutchinson, *Phys. Rev. A* **78**, 063614 (2008).
- [87] A. G. Sykes, M. J. Davis, and D. C. Roberts, *Phys. Rev. Lett.* **103**, 085302 (2009).
- [88] T. Paul, P. Schlagheck, P. Leboeuf, and N. Pavloff, *Phys. Rev. Lett.* **98**, 210602 (2007).
- [89] C. W. Gardiner and P. Zoller, *Quantum Noise* (Springer, New York, 2004).
- [90] C. W. Gardiner, *Handbook of Stochastic Methods* (Springer, Berlin, 1983).
- [91] P. D. Drummond and C. W. Gardiner, *J. Phys. A* **13**, 2353 (1980).
- [92] A. Gilchrist, C. W. Gardiner, and P. D. Drummond, *Phys. Rev. A* **55**, 3014 (1997).
- [93] P. Deuar and P. D. Drummond, *Phys. Rev. A* **66**, 033812 (2002).
- [94] M. Lewenstein and L. You, *Phys. Rev. Lett.* **77**, 3489 (1996).
- [95] Y. Castin and R. Dum, *Phys. Rev. A* **57**, 3008 (1998).